

Cyclooctatetraene Complexes of Yttrium and the Lanthanides with Bis(phosphinimino)methanides: Synthesis, Structure, and Hydroamination/Cyclization Catalysis¹

Tarun K. Panda, Agustino Zulys, Michael T. Gamer, and Peter W. Roesky*

Institut für Chemie, Freie Universität Berlin, Fabeckstrasse 34-36, 14195 Berlin, Germany

Received November 16, 2004

A series of cyclooctatetraene bis(phosphinimino)methanide complexes of yttrium and the lanthanides, $[\{\text{CH}(\text{PPh}_2\text{NSiMe}_3)_2\}\text{Ln}(\eta^8\text{-C}_8\text{H}_8)]$ (Ln = Y, Sm, Er, Yb, Lu), were synthesized via three different pathways. The title compounds can be obtained either from $[(\eta^8\text{-C}_8\text{H}_8)\text{-LnI}(\text{THF})_3]$ and $\text{K}\{\text{CH}(\text{PPh}_2\text{NSiMe}_3)_2\}$ or from $\text{K}_2\text{C}_8\text{H}_8$ and $[\{\text{CH}(\text{PPh}_2\text{NSiMe}_3)_2\}\text{LnCl}_2]_2$. In a third approach the title compounds were synthesized in a one-pot reaction starting from $\text{K}\{\text{CH}(\text{PPh}_2\text{NSiMe}_3)_2\}$, LnCl_3 , and $\text{K}_2\text{C}_8\text{H}_8$. All complexes have been characterized by crystal X-ray diffraction. The solid-state structures of these complexes show that both ligands completely shield the metal center. As a result of the steric crowding, both ligands are slightly asymmetrically attached to the metal. Even though the title compounds are noncharged lanthanide complexes with no obvious leaving group and no coordinated solvent molecules, the compounds were tested as catalysts for the hydroamination/cyclization reaction. A moderate catalytic activity at elevated temperature is observed.

Introduction

The catalytic addition of an organic amine $\text{R}_2\text{N-H}$ bond to alkenes or alkynes (hydroamination) to give nitrogen-containing molecules is of great interest for academic and industrial research, since most amines are made today in multistep syntheses.² In lanthanide chemistry amido and alkyl metallocene complexes have proven to be efficient catalysts for the hydroamination/cyclization of primary aminoolefines, allenes, and alkynes.³ Besides the well-established metallocenes today a number of non-cyclopentadienyl lanthanide complexes, which are based on amido and alkoxide ligands, are known to be active in the hydroamination/cyclization catalysis.^{4–9} The first non-cyclopentadienyl organolanthanide catalyst for the hydroamination/cyclization reaction was developed by us.⁴

Although it is well accepted today that cyclooctatetraene is beside cyclopentadienyl the most important π -perimeter ligand in f-element chemistry, there are almost no applications of cyclooctatetraene complexes as homogeneous catalyst.¹⁰ This is surprising since recently it was summarized in a review that the large flat cyclooctatetraene ligand represents an especially valuable alternative to the popular cyclopentadienyl ligands. Among non-cyclopentadienyl organolanthanide complexes, cyclooctatetraene derivatives form a large and well-investigated group of compounds.¹¹

In all metallocenes and non-cyclopentadienyl lanthanide catalysts for C–C multiple-bond transformation the cyclopentadienyl, amido, or alkoxide ligand acts as spectator ligand (L), whereas an alkyl or another amido group (R) is used as leaving group.^{2f} Thus, all these catalysts have the general composition L_2LnR or LLnR_2 . It was shown that the leaving group R is substituted by the substrate in the initial step of the catalytic reaction. Recently Collin and Trifonov reported that an

(1) Communication in part: Zulys, A.; Panda, T. K.; Gamer, M. T.; Roesky, P. W. *Chem. Commun.* **2004**, 2584–2585.

(2) Recent reviews: (a) Müller, T. E.; Beller, M. *Chem. Rev.* **1998**, *98*, 675–703. (b) Nobis, M.; Driessen-Hölscher, B. *Angew. Chem.* **2001**, *113*, 4105–4108; *Angew. Chem., Int. Ed.* **2001**, *40*, 3983–3985. (c) Müller, T. E. In *Encyclopedia of Catalysis*; Horváth, J. T., Ed.; Wiley: New York, 2002. (d) Pohlki, F.; Doye, S. *Chem. Soc. Rev.* **2003**, *32*, 104–114. (e) Roesky, P. W.; Müller, T. E. *Angew. Chem.* **2003**, *115*, 2812–2814; *Angew. Chem., Int. Ed.* **2003**, *42*, 2708–2710. (f) Hong, S.; Marks, T. J. *Acc. Chem. Res.* **2004**, *37*, 673–686.

(3) (a) Gagné, M. R.; Marks, T. J. *J. Am. Chem. Soc.* **1989**, *111*, 4108–4109. (b) Gagné, M. R.; Stern, C. L.; Marks, T. J. *J. Am. Chem. Soc.* **1992**, *114*, 275–294. (c) Li, Y.; Marks, T. J. *J. Am. Chem. Soc.* **1996**, *118*, 9295–9306. (d) Roesky, P. W.; Stern, C. L.; Marks, T. J. *Organometallics* **1997**, *16*, 4705–4711. (e) Li, Y.; Marks, T. J. *J. Am. Chem. Soc.* **1998**, *120*, 1757–1771. (f) Arredondo, V. M.; McDonald, F. E.; Marks, T. J. *J. Am. Chem. Soc.* **1998**, *120*, 4871–4872. (g) Arredondo, V. M.; Tian, S.; McDonald, F. E.; Marks, T. J. *J. Am. Chem. Soc.* **1999**, *121*, 3633–3639. (h) Hong, S.; Marks, T. J. *J. Am. Chem. Soc.* **2002**, *124*, 7886–7887. (i) Ryu, J.-S.; Li, G. Y.; Marks, T. J. *J. Am. Chem. Soc.* **2003**, *125*, 12584–12605.

(4) (a) Bürgstein, M. R.; Berberich, H.; Roesky, P. W. *Organometallics* **1998**, *17*, 1452–1454. (b) Bürgstein, M. R.; Berberich, H.; Roesky, P. W. *Chem. Eur. J.* **2001**, *7*, 3078–3085.

(5) (a) Kim, Y. K.; Livinghouse, T.; Bercaw, J. E. *Tetrahedron Lett.* **2001**, *42*, 2933–2935. (b) Kim, Y. K.; Livinghouse, T. *Angew. Chem.* **2002**, *114*, 3797–3799; *Angew. Chem., Int. Ed.* **2002**, *41*, 3645–3647. (c) Kim, Y. K.; Livinghouse, T.; Horino, Y. *J. Am. Chem. Soc.* **2003**, *125*, 9560–9561.

(6) (a) Gribkov, D. V.; Hultsch, K. C.; Hampel, F. *Chem. Eur. J.* **2003**, *9*, 4796–4810. (b) Hultsch, K. C.; Gribkov, D. V. *Chem. Commun.* **2004**, 730–731. (c) Hultsch, K. C.; Hampel, F.; Wagner, T. *Organometallics* **2004**, *23*, 2601–2612.

(7) Collin, J.; Daran, J.-C.; Schulz E.; Trifonov, A. *Chem. Commun.* **2003**, 3048–3049.

(8) Hong, S.; Tian, S.; Metz, M. V.; Marks, T. J. *J. Am. Chem. Soc.* **2003**, *125*, 14768–14783.

(9) O'Shaughnessy, P. N.; Knight, P. D.; Morton, C.; Gillespie, K. M.; Scott, P. *Chem. Commun.* **2003**, 1770–1771.

(10) Edelmann, F. T. *Angew. Chem.* **1995**, *107*, 2647–2669; *Angew. Chem., Int. Ed. Engl.* **1995**, *34*, 2466–2488.

(11) Edelmann, F. T.; Freckmann D. M. M.; Schumann H. *Chem. Rev.* **2002**, *102*, 1851–1896.

anionic bis(binaphthylidiamino) ytterbium complex, which has no obvious leaving group, can act as catalyst for the hydroamination/cyclization reaction. Unfortunately no detailed studies on the mechanism were presented, but it seems reasonable either that one of the binaphthylidiamino ligands leaves during the reaction or that an ionic mechanism takes place. On the basis of these observations we were curious to see if a noncharged lanthanide complex with no obvious leaving group and no coordinated solvent molecule, which could diffuse off from the metal center, may also act as catalyst for the hydroamination/cyclization reaction.⁷ Therefore, we desired to synthesize lanthanides complexes in which the metal center is completely shielded by ligands, which stay attached under catalytic conditions.

Herein we report on a cyclooctatetraene bis(phosphinimino)methanide complex of yttrium and the lanthanides [$\{\text{CH}(\text{PPh}_2\text{NSiMe}_3)_2\}\text{Ln}(\eta^8\text{-C}_8\text{H}_8)\}$]. In these compounds the metal center is completely shielded by two very bulky ligands. Nevertheless a moderate activity of these compounds in the hydroamination/cyclization is observed. In this contribution, we present a full account of the reaction scope, substrate selectivity, lanthanide ion size effect, and some kinetic/mechanistic aspects of the hydroamination/cyclization catalyzed by [$\{\text{CH}(\text{PPh}_2\text{NSiMe}_3)_2\}\text{Ln}(\eta^8\text{-C}_8\text{H}_8)\}$].

Experimental Section

General Procedures. All manipulations of air-sensitive materials were performed with the rigorous exclusion of oxygen and moisture in flame-dried Schlenk-type glassware either on a dual manifold Schlenk line, interfaced to a high vacuum (10^{-4} Torr) line, or in an argon-filled M. Braun glovebox. Ether solvents (tetrahydrofuran and ethyl ether) were predried over Na wire and distilled under nitrogen from K (THF) or Na wire (ethyl ether) benzophenone ketyl prior to use. Hydrocarbon solvents (toluene and *n*-pentane) were distilled under nitrogen from LiAlH_4 . All solvents for vacuum-line manipulations were stored in vacuo over LiAlH_4 in resealable flasks. Deuterated solvents were obtained from Chemotrade Chemiehandelsgesellschaft mbH (all ≥ 99 atom % D) and were degassed, dried, and stored in vacuo over Na/K alloy in resealable flasks. NMR spectra were recorded on a Bruker AC 250 or JNM-LA 400 FT-NMR spectrometer. Chemical shifts are referenced to internal solvent resonances and are reported relative to tetramethylsilane and 85% phosphoric acid (^{31}P NMR), respectively. Elemental analyses were carried out with an Elementar Vario EL. LnCl_3 ,¹² [$(\text{C}_8\text{H}_8)\text{-SmI}(\text{THF})_3$],¹³ $\text{K}\{\text{CH}(\text{PPh}_2\text{NSiMe}_3)_2\}$,¹⁴ and [$\{\text{CH}(\text{PPh}_2\text{NSiMe}_3)_2\}\text{SmCl}_2$]¹⁵ were prepared according to literature procedures.

[$\{\text{CH}(\text{PPh}_2\text{NSiMe}_3)_2\}\text{Sm}(\eta^8\text{-C}_8\text{H}_8)$] (1b). Route A.¹ A 20 mL portion of THF was condensed at -196°C onto a mixture of 200 mg (0.33 mmol) of $\text{K}\{\text{CH}(\text{PPh}_2\text{NSiMe}_3)_2\}$ and 185 mg (0.31 mmol) of [$(\text{C}_8\text{H}_8)\text{SmI}(\text{THF})_3$]. The mixture was stirred for 18 h at room temperature and filtered. The solvent was then evaporated in vacuo and toluene condensed onto the mixture. The mixture was refluxed for a short period and filtered, and the solvent was taken off in vacuo. The product was recrystallized from THF/*n*-pentane (1:2): red crystals. Yield: 84%.

(12) Taylor, M. D.; Carter, C. P. *J. Inorg. Nucl. Chem.* **1962**, *24*, 387–391.

(13) Mashima, K.; Nakayama, Y.; Nakamura, A.; Kanehisa, N.; Kai, T.; Takaya, H. *J. Organomet. Chem.* **1994**, *473*, 85–91.

(14) Gamer, M. T.; Roesky, P. W. *Z. Anorg. Allg. Chem.* **2001**, *627*, 877–881.

(15) Gamer, M. T.; Dehnen S.; Roesky, P. W. *Organometallics* **2001**, *20*, 4230–4236.

Route B.¹ A solution of 381 mg (0.25 mmol) of [$\{\text{CH}(\text{PPh}_2\text{NSiMe}_3)_2\}\text{SmCl}_2$] in 10 mL of THF was added to a freshly prepared solution of 0.49 mmol of $\text{K}_2\text{C}_8\text{H}_8$ in THF, and the mixture was stirred for 18 h at room temperature. The solvent was then evaporated in vacuo and 50 mL of toluene condensed onto the mixture. The mixture was filtered, and the solvent removed under vacuum. The product was recrystallized from THF/*n*-pentane (1:2). Yield: 78%. IR (KBr [cm^{-1}]): 3017(m), 1436(s), 1260(s), 1240(s), 1155(m), 1107(m), 985(s), 919(s), 843(m), 748(m), 690(m), 616(s), 589(s), 559(s), 515(s), 505(m). ^1H NMR (C_6D_6 , 400 MHz, 25°C): δ -0.06 (s, 18H, SiMe_3), 3.87 (br, 1H, CH), 6.37–6.43 (m, 4H, Ph), 6.51 (br, 4H, Ph), 6.60–6.66 (m, 2H, Ph), 7.38–7.44 (m, 2H, Ph), 7.62–7.68 (m, 4H, Ph), 9.74 (br, 4H, Ph), 10.73 (s, 8H, C_8H_8). ^{29}Si NMR (C_6D_6 , 49.7 MHz, 25°C): δ 4.4 ppm. $^{31}\text{P}\{\text{H}\}$ NMR (C_6D_6 , 161.7 MHz, 25°C): δ 56.1. Anal. Calcd for $\text{C}_{39}\text{H}_{47}\text{N}_2\text{P}_2\text{Si}_2\text{Sm}$ (812.29): C 57.67, H 5.83, N 3.45. Found: C 57.42, H 5.93, N 3.43.

General Route for [$\{\text{CH}(\text{PPh}_2\text{NSiMe}_3)_2\}\text{Ln}(\eta^8\text{-C}_8\text{H}_8)$] ($\text{Ln} = \text{Y}$ (1a), Sm (1b), Er (1c), Yb (1d), Lu (1e)). The reaction was done in a one-pot synthesis. Anhydrous LnCl_3 (1.1 mmol) was mixed with 597 mg (1 mmol) of $\text{K}\{\text{CH}(\text{PPh}_2\text{NSiMe}_3)_2\}$ under an inert atmosphere. THF (15 mL) was condensed onto it. The reaction solution was allowed to warm to room temperature and kept stirring for 24 h. To this solution was added a THF solution of freshly prepared $\text{K}_2(\text{C}_8\text{H}_8)$ (1 mmol) at room temperature. Immediately a color change was observed. The solution was kept under stirring conditions for a further 20 h. THF was removed in vacuo. The residue was dissolved in 15 mL of toluene and filtered. Toluene was evaporated, and the compound was washed with 10 mL of pentane. Finally, the title compounds were crystallized from either THF/pentane (1:3) or hot toluene.

$\text{Ln} = \text{Y}$: red crystals. Yield: 74%. ^1H NMR (C_6D_6 , 400 MHz, 25°C): δ 0.23 (s, 18H, SiMe_3), 1.30 (br, 1H, CH), 6.54 (s, 8H, C_8H_8), 6.57–6.63 (m, 4H, Ph), 6.71–6.74 (m, 4H, Ph), 7.01 (br, 2H, Ph), 7.05–7.10 (m, 2H, Ph), 7.67 (br, 4H, Ph), 7.79–7.83 (m, 4H, Ph). $^{31}\text{P}\{\text{H}\}$ NMR (C_6D_6 , 161.7 MHz 25°C): δ 16.8 (d, $^2J(\text{P,Y}) = 6.0$ Hz). Anal. Calcd for $\text{C}_{39}\text{H}_{47}\text{N}_2\text{P}_2\text{Si}_2\text{Y}$ (750.83): C 62.39, H 6.31, N 3.73. Found: C 61.49, H 6.55, N 3.18.

$\text{Ln} = \text{Sm}$. Yield: 70%.

$\text{Ln} = \text{Er}$: pink crystals. Yield: 60%. Anal. Calcd for $\text{C}_{39}\text{H}_{47}\text{ErN}_2\text{P}_2\text{Si}_2$ (829.19): C 56.49, H 5.71, N 3.38. Found: C 55.56, H 5.86, N 3.23. FT Raman (single crystal cm^{-1}): 248(m), 277(s), 297(br), 616(s), 682(br), 691(s), 998(s), 1028(s), 1109(br), 1160(br), 1182(br), 1573(s), 1590(s), 3058(s).

$\text{Ln} = \text{Yb}$: green crystals. Yield: 65%. Anal. Calcd for $\text{C}_{83}\text{H}_{104}\text{Yb}_2\text{N}_4\text{P}_4\text{Si}_4$ (1740.05) [= (2 **1e**)·(pentane)]: C 57.29, H 6.02, N 3.22. Found: C 56.74, H 6.15, N 3.24. FT Raman (single crystal cm^{-1}): 241(m), 294(s), 616(s), 683(br), 690(s), 997(s), 1028(s), 1108(br), 1167(br), 1188(br), 1484(br), 1590(s), 2915(br), 2982(br), 3057(s).

$\text{Ln} = \text{Lu}$: yellow crystals. Yield: 75%. ^1H NMR (C_6D_6 , 400 MHz, 25°C): δ 0.25 (s, 18H, SiMe_3), 1.30 (br, H, CH), 6.49 (s, 8H, C_8H_8), 6.60–6.61 (m, 4H, Ph), 6.70–6.72 (m, 4H, Ph), 7.01–7.02 (m, 2H, Ph), 7.05–7.08 (m, 2H, Ph), 7.65–7.69 (m, 4H, Ph), 7.82 (br, 4H, Ph). $^{31}\text{P}\{\text{H}\}$ NMR (C_6D_6 , 161.7 MHz, 25°C): δ 20.2. Anal. Calcd for $\text{C}_{83}\text{H}_{104}\text{Lu}_2\text{N}_4\text{P}_4\text{Si}_4$ (1743.88) [= (2 **1e**)·(pentane)]: C 57.16, H 6.01, N 3.21. Found: C 57.73, H 6.35, N 3.05.

General Procedure for the Hydroamination Reaction (NMR Scale Reaction). Compound **1** was weighed under argon gas into an NMR tube. C_6D_6 (~0.7 mL) was condensed into the NMR tube, and the mixture was frozen to -196°C . The reactant was injected onto the solid mixture, and the whole sample was melted and mixed just before the insertion into the core of the NMR machine (t_0). The ratio between the reactant and the product was exactly calculated by comparison of the integration of the corresponding signals.

X-ray Crystallographic Studies of 1a–e. Crystals of **1a–f** were grown from THF/pentane (1:3) or hot toluene. A suitable crystal was covered in mineral oil (Aldrich) and

Table 1. Crystallographic Details for $\{[\text{CH}(\text{PPh}_2\text{NSiMe}_3)_2]\text{Ln}(\eta^8\text{-C}_8\text{H}_8)\}$ (1a–e**)^a**

	(2 1a)·(pentane)	1b	(2 1c)·(pentane)
formula	C ₈₃ H ₁₀₄ N ₄ P ₄ Si ₄ Y ₂	C ₃₉ H ₄₇ N ₂ P ₂ Si ₂ Sm	C ₈₃ H ₁₀₄ Er ₂ N ₄ P ₄ Si ₄
fw	1571.76	812.26	1728.46
space group	<i>P</i> $\bar{1}$ (No. 2)	<i>P</i> 2 ₁ / <i>n</i> (No. 14)	<i>P</i> $\bar{1}$ (No. 2)
<i>a</i> , Å	9.402(2)	12.3050(8)	9.379(2)
<i>b</i> , Å	9.530(2)	19.6230(13)	9.490(2)
<i>c</i> , Å	22.771(4)	15.6500(10)	22.693(4)
α , deg	93.146(4)		93.345(4)
β , deg	92.938(4)	99.364(8)	92.875(4)
γ , deg	98.530(4)		98.921(4)
<i>V</i> , Å ³	2011.1(6)	3728.5(4)	1988.3(6)
<i>Z</i>	1	4	1
density (g/cm ³)	1.298	1.447	1.444
radiation	Mo K α ($\lambda = 0.71073$ Å)	Ag K α ($\lambda = 0.56087$ Å)	Mo K α ($\lambda = 0.71073$ Å)
μ , mm ⁻¹	1.620	0.938	2.282
absorption correction	Empirical (SADABS)	none	Empirical (SADABS)
refl. collected	25 111	24 303	24 365
unique refls	12 116 [<i>R</i> _{int} = 0.0183]	7714 [<i>R</i> _{int} = 0.1285]	11 911 [<i>R</i> _{int} = 0.0189]
obsd refls	10 132	5976	10 569
data; params	12 116; 437	7714; 421	11 911; 437
<i>R</i> ₁ ^b ; <i>wR</i> ₂ ^c	0.0341; 0.0949	0.0585; 0.1742	0.0262; 0.0653

	(2 1d)·(pentane)	(2 1e)·(pentane)
formula	C ₈₃ H ₁₀₄ N ₄ P ₄ Si ₄ Yb ₂	C ₈₃ H ₁₀₄ Lu ₂ N ₄ P ₄ Si ₄
fw	1740.02	1743.88
space group	<i>P</i> $\bar{1}$ (No. 2)	<i>P</i> $\bar{1}$ (No. 2)
<i>a</i> , Å	9.377(2)	9.351(2)
<i>b</i> , Å	9.508(2)	9.500(2)
<i>c</i> , Å	22.703(5)	22.700(5)
α , deg	93.493(4)	93.619(5)
β , deg	92.759(4)	92.852(5)
γ , deg	99.268(4)	99.437(5)
<i>V</i> , Å ³	1990.6(7)	1981.7(7)
<i>Z</i>	1	1
density (g/cm ³)	1.451	1.461
radiation	Mo K α ($\lambda = 0.71073$ Å)	Mo K α ($\lambda = 0.71073$ Å)
μ , mm ⁻¹	2.521	2.663
absorption correction	Empirical (SADABS)	Empirical (SADABS)
refl. collected	24 561 [<i>R</i> _{int} = 0.0195]	23 438 [<i>R</i> _{int} = 0.0189]
unique refls	11 939	11 918
obsd refls	10 682	10 971
data; params	11 939; 437	11 918; 437
<i>R</i> ₁ ^b ; <i>wR</i> ₂ ^c	0.0265; 0.0670	0.0237; 0.0605

^a All data collected at 203 K. ^b $R_1 = \sum ||F_o| - |F_c|| / \sum |F_o|$. ^c $wR_2 = \{\sum [w(F_o^2 - F_c^2)^2] / \sum [w(F_o^2)^2]\}^{1/2}$.

mounted onto a glass fiber. The crystal was transferred directly to the -73 °C cold N₂ stream of a Stoe IPDS or a Bruker Smart 1000 CCD diffractometer. Subsequent computations were carried out on an Intel Pentium III PC or Intel Pentium IV PC.

All structures were solved by the Patterson method (SHELXS-97¹⁶). The remaining non-hydrogen atoms were located from successive difference Fourier map calculations. The refinements were carried out by using full-matrix least-squares techniques on *F*, minimizing the function $(F_o - F_c)^2$, where the weight is defined as $4F_o^2/2(F_o^2)$ and *F*_o and *F*_c are the observed and calculated structure factor amplitudes using the program SHELXL-97.¹⁷ In the final cycles of each refinement, all non-hydrogen atoms except the pentane molecules in **1a** and **1c–1e** were assigned anisotropic temperature factors. Carbon-bound hydrogen atom positions were calculated and allowed to ride on the carbon to which they are bonded assuming a C–H bond length of 0.95 Å. The hydrogen atom contributions were calculated, but not refined. The final values of refinement parameters are given in Table 1. The

locations of the largest peaks in the final difference Fourier map calculation as well as the magnitude of the residual electron densities in each case were of no chemical significance. Positional parameters, hydrogen atom parameters, thermal parameters, and bond distances and angles have been deposited as Supporting Information. Crystallographic data (excluding structure factors) for the structures reported in this paper have been deposited with the Cambridge Crystallographic Data Centre as supplementary publication nos. CCDC-253386 (**1a**), 242557 (**1b**), 253387 (**1c**), 253388 (**1d**), and 253389 (**1e**). Copies of the data can be obtained free of charge on application to CCDC, 12 Union Road, Cambridge CB21EZ, UK (fax: +44)1223-336-033; e-mail: deposit@ccdc.cam.ac.uk).

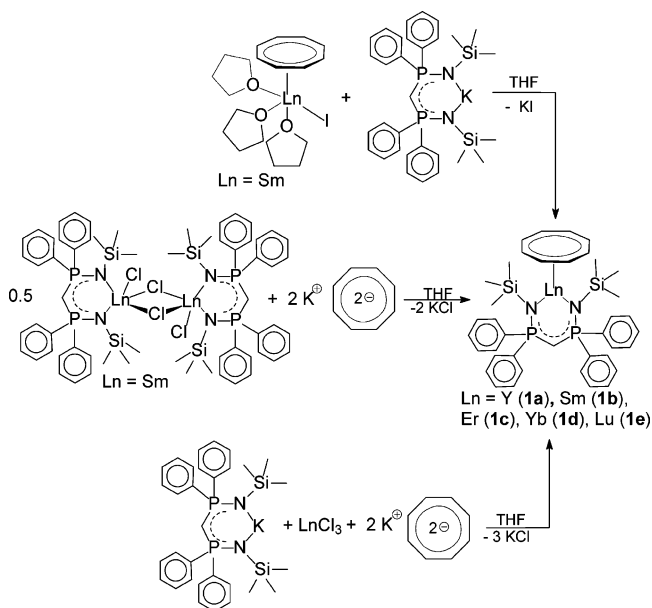
Results and Discussion

The Metal Complexes. The title compounds $\{[\text{CH}(\text{PPh}_2\text{NSiMe}_3)_2]\text{Ln}(\eta^8\text{-C}_8\text{H}_8)\}$ (Ln = Y (**1a**), Sm (**1b**), Er (**1c**), Yb (**1d**), Lu (**1e**)) can be obtained by three different synthetic approaches. All approaches were performed for the samarium complex **1b**, whereas the other complexes were obtained in a one-pot reaction only. The first approach starts from the well-established compound $[(\eta^8\text{-C}_8\text{H}_8)\text{SmI}(\text{THF})_3]$,¹³ which was reacted with

(16) Sheldrick, G. M. *SHELXS-97, Program of Crystal Structure Solution*, University of Göttingen, Germany, 1997.

(17) Sheldrick, G. M. *SHELXL-97, Program of Crystal Structure Refinement*, University of Göttingen, Germany, 1997.

Scheme 1



$\text{K}\{\text{CH}(\text{PPh}_2\text{NSiMe}_3)_2\}$,¹⁴ in a 1:1 molar ratio in THF at room temperature to afford the corresponding bis-(phosphinimino)methanide complex **1b** (Scheme 1).¹⁸ Compound **1b** was also obtained by a reaction of $\text{K}_2\text{C}_8\text{H}_8$ with bis(phosphinimino)methanide samarium dichloride $[\{\text{CH}(\text{PPh}_2\text{NSiMe}_3)_2\}\text{SmCl}_2]_2$ ¹⁵ in THF in a 2:1 molar ratio (Scheme 1).¹⁸ However, the most convenient approach to **1a–e** is a one-pot reaction, in which the potassium methanide complex, $\text{K}\{\text{CH}(\text{PPh}_2\text{NSiMe}_3)_2\}$,¹⁴ is reacted with anhydrous yttrium or lanthanide trichlorides in a 1:1.1 molar ratio in THF followed by addition of a freshly prepared solution of 1 equiv of $\text{K}_2\text{C}_8\text{H}_8$ in THF (Scheme 1).¹⁸

The new complexes have been characterized by standard analytical/spectroscopic techniques, and the solid-state structures of all five compounds were established by single-crystal X-ray diffraction. The ^1H NMR spectra of the diamagnetic compounds **1a,e** show typical sharp singlets for the cyclooctatetraene ring (δ 6.54 (**1a**), 6.49 ppm (**1e**)) and the Me_3Si group of the bis(phosphinimino)methanide ligand (δ 0.23 (**1a**), 0.25 ppm (**1e**)). The chemical shift of methine protons is more sensitive to the chemical surrounding. It shows an upfield shift (δ 1.3 (**1a**), 1.3 (**1e**)) compared to the chlorine precursor $[\{\text{CH}(\text{PPh}_2\text{NSiMe}_3)_2\}\text{LnCl}_2]_2$ (δ 1.93 (Ln = Y), 1.97 (Ln = Lu)). The $^2J(\text{H},\text{P})$ coupling constant of the methine proton is very small; thus only a broadening of the signals is observed. The signals of the phenyl protons are broadened in the ^1H NMR spectrum.

Complexes **1a,e** each show a sharp signal in the $^{31}\text{P}\{-^1\text{H}\}$ NMR spectra (δ 16.8 (**1a**), 20.2 (**1e**)) and are in the range of $[\{\text{CH}(\text{PPh}_2\text{NSiMe}_3)_2\}\text{LnCl}_2]_2$ (δ 20.4 (Ln = Y), 20.5 (Ln = Lu)), showing that the phosphorus atoms in each case are chemically equivalent in solution. In the $^{31}\text{P}\{-^1\text{H}\}$ NMR spectrum of **1a**, a $^2J(\text{P},\text{Y})$ coupling of 6.0 Hz is observed. Also for **1b**, ^1H , ^{29}Si , and ^{31}P NMR spectra were obtained, which are quantitatively comparable to those of **1a,e**. Nevertheless, due to the influence of the paramagnetic samarium center, the

observed chemical shifts are significantly different. Thus, the signal in the ^{31}P NMR is observed at δ ($^{31}\text{P}\{-^1\text{H}\}$) 56.1 ppm, and in the ^1H NMR spectrum of **1b** the characteristic singlet for the $\text{C}_8\text{H}_8^{2-}$ ring is at low field (δ 10.73 ppm). The data obtained are in good agreement with earlier observations. Thus, the signals of the $\text{C}_8\text{H}_8^{2-}$ ring in known samarium compounds are shifted over a wide range, e.g., δ 9.33 ppm in $[(\eta^8\text{-C}_8\text{H}_8)\text{Sm}\{(i\text{Pr})_2\text{ATI}\}(\text{THF})]^{19}$ ($(i\text{Pr})_2\text{ATI}$ = *N*-isopropyl-2-(isopropylamino)troponimate), δ 13.2 ppm in $[\text{Li}(\text{THF})_3\{\mu\text{-}(\eta^2\text{-}\eta^8\text{-C}_8\text{H}_8)\}\text{Sm}(\eta^8\text{-C}_8\text{H}_8)]$,²⁰ and δ 13.5 ppm in $[(\eta^8\text{-C}_8\text{H}_8)\text{-Sm}(\text{hmpa})_3][(\eta^8\text{-C}_8\text{H}_8)_2\text{Sm}]$.²¹

The structures of **1a–e** were confirmed by single-crystal X-ray diffraction in the solid state. Data collection parameters and selected bond lengths and angles are given in Tables 1 and 2. Due to the similar ion radii of the lanthanides, the single-crystal X-ray structures of **1a–e** are similar. As a representative example, the structure of **1e** is shown in Figure 1. As a result of the larger ion radius, the samarium complex **1b** crystallizes in the monoclinic space group $P2_1/n$, whereas all other compounds crystallize in the triclinic space group $P\bar{1}$ with a molecule of *n*-pentane in the unit cell. The coordination polyhedron is formed by the η^8 -coordinated cyclooctatetraene ring and the $\{\text{CH}(\text{PPh}_2\text{NSiMe}_3)_2\}^-$ ligand. Since both ligands are very bulky, a steric crowding around the metal center is observed. Consequently, in contrast to most other cyclooctatetraene complexes of the lanthanides, no solvent molecule is attached to the metal. Furthermore, as a result of the high steric crowding, both ligands are slightly asymmetrically bound to the lanthanide atom. Thus, for the cyclooctatetraene ring the Ln–C bond lengths to the eight-membered ring vary over the wide range of (2.571(2)–2.627(2) Å (av 2.595 Å) (**1a**), 2.594(7)–2.675(5) (av 2.647 Å) (**1b**), 2.560(3)–2.608(3) Å (av 2.579 Å) (**1c**), 2.538(3)–2.596(3) Å (av 2.563 Å) (**1d**), and 2.525(3)–2.593(2) Å (av 2.555 Å) (**1e**)). In addition to the cyclooctatetraene ring, the $\{\text{CH}(\text{PPh}_2\text{NSiMe}_3)_2\}^-$ ligand is asymmetrically attached to the metal. Thus, the Ln–N1 distances (2.4163(14) Å (**1a**), 2.533(4) Å (**1b**), 2.393(2) Å (**1c**), 2.371(2) Å (**1d**), 2.362(2) Å (**1e**)) are significantly longer than the Ln–N2 distances (2.3899(14) Å (**1a**), 2.458(4) Å (**1b**), 2.3641(2) Å (**1c**), 2.3451(2) Å (**1d**), 2.334(2) Å (**1e**)). A six-membered metallacycle (N1–P1–C9–P2–N2–Ln) is formed by chelation of the two trimethylsilylimine groups to the lanthanide atom. The ring adopts a twist boat conformation, in which the central carbon atom and the lanthanide atom are displaced from the N_2P_2 least-squares plane. The distance between the central carbon atom (C9) and the lanthanide atom (2.7654(2) Å (**1a**), 2.724(5) Å (**1b**), 2.737(2) Å (**1c**), 2.711(2) Å (**1d**), 2.693(2) Å (**1e**)) is longer than usual Ln–C distances; however resultant tridentate coordination of the ligand was observed earlier.^{15,22} The folding of the six-membered metallacycle seems to depend mainly on the packing in the solid state and not on the ion radius of the lanthanide metal. The angle $\text{C}_g\text{-Ln-C9}$ (C_g , ring centroid) is in the range of 140° for all complexes, which crystallize in the triclinic space

(19) Roesky, P. W. *J. Organomet. Chem.* **2001**, *621*, 277–283.(20) Wetzel, T. G.; Dehnen, S.; Roesky, P. W. *Organometallics* **1999**, *18*, 3835–3842.(21) Mashima, K.; Fukumoto, H.; Nakayama, Y.; Tani, K.; Nakamura, A. *Polyhedron* **1998**, *17*, 1065–1071.

(18) The bonding situation in the drawings of the ligand system in eqs 1 and 2 is simplified for clarity.

Table 2. Selected Bond Lengths and Angles of $[\{\text{CH}(\text{PPh}_2\text{NSiMe}_3)_2\text{Ln}(\eta^8\text{-C}_8\text{H}_8)\}]$ (**1a–e**)

	1a	1b	1c	1d	1e
Bond Lengths (Å)					
Ln–N1	2.4163(14)	2.533(4)	2.393(2)	2.371(2)	2.362(2)
Ln–N2	2.3899(14)	2.458(4)	2.3641(2)	2.3451(2)	2.334(2)
Ln–C9	2.7654(2)	2.724(5)	2.737(2)	2.711(2)	2.693(2)
C _g ^a –Ln	1.839(4)	1.914(1)	1.813(4)	1.794(4)	1.780(5)
C9–P1	1.738(2)	1.723(4)	1.738(2)	1.739(2)	1.735(2)
C9–P2	1.7517(2)	1.741(4)	1.750(2)	1.749(2)	1.751(2)
N1–P1	1.5936(15)	1.599(4)	1.594(2)	1.593(2)	1.591(2)
N2–P2	1.6091(14)	1.592(4)	1.612(2)	1.607(2)	1.609(2)
Bond Angles (deg)					
C _g –Ln–N1	132.31(1)	138.78(1)	132.01(1)	131.79(1)	131.70(1)
C _g –Ln–N2	136.51(1)	131.6(1)	136.04(1)	135.73(5)	135.63(1)
C _g –Ln–C9	140.15(1)	131.96(1)	139.99(1)	139.43(4)	139.80(1)
N1–Ln–N2	89.25(5)	89.60(13)	89.82(7)	90.35(7)	90.16(6)
N1–Ln–C9	62.01(5)	61.47(13)	62.60(6)	63.24(6)	63.30(6)
N2–Ln–C9	63.82(5)	63.16(13)	64.46(6)	64.86(7)	65.37(6)
P1–N1–Ln	98.93(7)	96.7(2)	98.71(9)	98.45(9)	98.41(9)
P2–N2–Ln	101.28(6)	100.0(2)	101.05(9)	100.97(9)	100.59(8)
N1–P1–C9	107.37(8)	108.2(2)	107.14(10)	107.03(11)	106.57(10)
N2–P2–C9	109.38(7)	109.5(2)	109.07(10)	108.78(10)	108.68(9)

^a C_g, ring centroid.

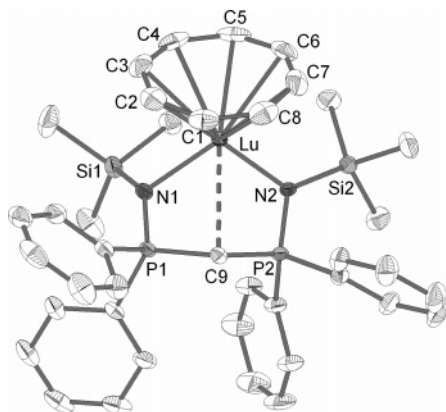


Figure 1. Perspective ORTEP view of the molecular structure of **1e**. Thermal ellipsoids are drawn to encompass 50% probability. Hydrogen atoms are omitted for clarity.

group (140.15(1)° (**1a**), 139.99(1)° (**1c**), 139.43(4)° (**1d**), 139.80(1)° (**1e**)), whereas for **1b**, which crystallizes as a monoclinic system, only C_g–Ln–C9 131.96(1)° is observed.

Hydroamination/Cyclization Catalysis. The mechanism of the lanthanide metallocene-catalyzed hydroamination/cyclization reaction was established some years ago by Marks et al.^{2f} In the initial step of this mechanism a leaving group on the metallocene precatalyst is replaced by the substrate. Recently, some non-cyclopentadienyl lanthanide catalysts for the hydroamination/cyclization were reported.^{4–6} Some of these complexes show a significant activity only at elevated temperature over a long period.⁵ In this context we were curious to see if the sluggish reactivity is just a matter of the activation barrier in the established mechanism

or if some other mechanistic aspect may be involved. Therefore, we used compounds **1**, which are noncharged lanthanide complexes with no obvious leaving group and no coordinated solvent molecule, as catalysts for the hydroamination/cyclization reaction.

The scope and the limitation by using **1** as catalyst in the intramolecular hydroamination/cyclization reaction were tested with different aminoalkynes and aminoolefins. The results are summarized in Table 3. No reaction was observed at room temperature (entry 2), but a moderate activity with sometimes quantitative yields is seen at elevated temperature. The reaction scope is limited so far on five-membered ring formation. The rigorously anaerobic reaction of the catalysts with dry, degassed aminoolefin and aminoalkynes (catalyst: substrate ≈ 1:50) proceeds regioselectively (>95%) in benzene. As observed for the metallocene catalyst of the lanthanides, the yields and the rates are dependent on the ion radius of the center metal (entries 1, 3, 5, and 6). Due to the similar ion radius of Yb³⁺ and Lu³⁺, compound **1d** was not investigated. As test reaction the cyclization of 5-phenyl-4-pentyn-1-amine to the corresponding 3,4-dihydropyrrole was used (Figure 2). The two aminoalkynes were converted to the cyclic product at elevated temperature in quantitative yields (entries 3 and 8). In contrast aminoolefins could be reacted only if they have geminal bulky substituents in the β-position to the amino group (Thorpe–Ingold effect)²³ (entries 9, 10, and 11).

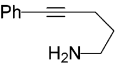
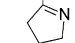
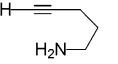
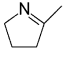
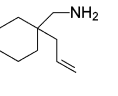
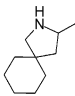
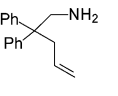
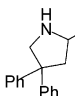
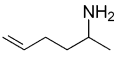
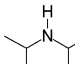
Kinetic studies were undertaken by in situ ¹H NMR spectroscopy. The reaction of a 50-fold molar excess of the substrates was monitored with constant catalyst concentration until complete substrate consumption. The decrease of the substrate peak was integrated versus the product signals. Figure 2 presents kinetics data for the cyclization of 5-phenyl-4-pentyn-1-amine with different catalysts, which indicates zero-order kinetics in substrate concentration, in an analogy with the results of the metallocene catalysts.

To probe the stability of **1b** under catalytic conditions, the reaction was performed with high catalyst concen-

(22) (a) Imhoff, P.; Guelpen, J. H.; Vrieze, K.; Smeets, W. J. J.; Spek, A. L.; Elsevier, C. J. *Inorg. Chim. Acta* **1995**, *235*, 77–88. (b) Ong, C. M.; McKarns, P.; Stephan, D. W. *Organometallics* **1999**, *18*, 4197–4208. (c) Kasani, A.; Kamalesh Babu, R. P.; McDonald, R.; Cavell, R. G. *Organometallics* **1999**, *18*, 3775–3777. (d) Aparna, K.; McDonald, R.; Ferguson, M.; Cavell, R. G. *Organometallics* **1999**, *18*, 4241–4243. (e) Wei, P.; Stephan, D. W. *Organometallics* **2002**, *21*, 1308–1310. (f) Gamer, M. T.; Roesky, P. W. *J. Organomet. Chem.* **2002**, *647*, 123–127. (g) Sarsfield, M. J.; Steele, H.; Helliwell, M.; Teat, S. J. *Dalton Trans.* **2003**, 3443–3449. (h) Hill, M. S.; Hitchcock, P. B. *Dalton Trans.* **2003**, 4570–4571. (i) Bibal, C.; Pink, M.; Smurnyy, Y. D.; Tomaszewski, J.; Caulton, K. G. *J. Am. Chem. Soc.* **2004**, *126*, 2312–2313.

(23) Kirby, A. J. *Adv. Phys. Org. Chem.* **1980**, *17*, 183–278.

Table 3. Hydroamination/Cyclization Reaction of Terminal Aminoolefines and Alkynes^a

Entry	Substrate	Prod.	Cat.	T °C	Yield % ^{b)}	Nt [h ⁻¹]
1			1a	120	quant.	0.36
2			1b	20	-	-
3			1b	120	quant.	0.60
4			1b^{c)}	120	quant.	0.38
5			1c	120	quant.	2.26
6			1d	120	87	0.40
7			2	20	quant.	3.3 ^{d)}
8			1b	120	quant.	1.54
9			1b	120	44	0.13
10			1c	120	56	0.20
11			1b	120	75	0.19
12			1b	120	-	-

^a 0.6 mmol substrate; 2 mol % of **1**, solvent: C₆D₆ in a sealed NMR tube. ^b Determined by ¹H NMR. ^c 6 mol % of **1**. ^d Ref 4a.

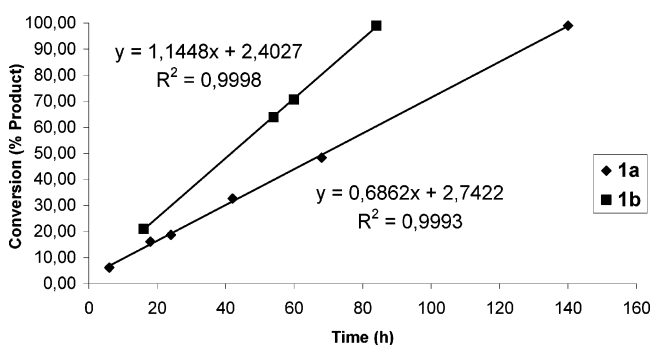


Figure 2. Ratio of conversion to lanthanide concentration as a function of time for the hydroamination/cyclization of 5-phenyl-4-pentyn-1-amine using compounds **1a** and **1b** as catalysts in benzene.

trations on the NMR scale. As a result of the paramagnetic shifts of the NMR signals of the samarium

compound **1b**, a dissociation of the {CH(PPh₂NSiMe₃)₂}⁻ ligand can easily be monitored by ³¹P{¹H} NMR spectroscopy, whereas the signal of the cyclooctatetraene ring shifts upon dissociation from δ 10.73 ppm in the normal olefin region. These experiments showed that neither the bis(phosphinimino)methanide ligand nor the cyclooctatetraene ring is cleaved off from the catalyst. To support these results, compound **1b** was heated in benzene in the presence of dry *n*-butylamine for 7 days. Under these conditions only a slight decomposition was observed.

Compound **1** cannot compete with the well-established metallocene catalysts such as Cp₂*YCH(SiMe₃)₂ (**2**)³ (entry 7), but it shows a new mechanistic pathway of the hydroamination/cyclization reaction. Even a good leaving group seems to increase the rate of the catalysis significantly. The reaction obviously also works in some cases in the absence of such a leaving group, although we cannot absolutely exclude that a vacant coordination site, which causes catalytic activity, is generated by some decomposition or some dynamic process within the coordination sphere of **1**.

Summary

In summary, we have prepared a series of cyclooctatetraene bis(phosphinimino)methanide complexes of yttrium and the lanthanides [{CH(PPh₂NSiMe₃)₂}Ln(η⁸-C₈H₈)] by three different approaches. The single-crystal X-ray structures of these complexes show that both ligands completely shield the metal center. As a result of the steric crowding, both ligands are slightly asymmetrically attached to the metal. Even though the title compounds are noncharged lanthanide complexes with no obvious leaving group and no coordinated solvent molecules, the compounds were tested as catalyst for the hydroamination/cyclization reaction. A moderate catalytic activity at elevated temperature is observed. The obtained results do not fit into the previously established mechanism for the hydroamination/cyclization reaction, in which a leaving group on the precatalyst is replaced by the substrate in the initial step. Thus, a prolonged heating of a lanthanide-catalyzed hydroamination/cyclization reaction may open, besides the established mechanisms, an alternative reaction pathway.

Acknowledgment. This work was supported by the Deutsche Forschungsgemeinschaft and the Fonds der Chemischen Industrie. We thank Prof. Dr. G. Schröder (Karlsruhe) for the gift of cyclooctatetraene. Additionally, the generous support from Prof. Dr. D. Fenske is gratefully acknowledged.

Supporting Information Available: X-ray crystallographic files in CIF format for the structure determinations of **1a–e** are available free of charge via the Internet at <http://pubs.acs.org>.

OM0491138